# Determination of the Chemical Shielding Tensor Orientation from Two or One of the Three Conventional Rotations of a Single Crystal

S. C. Shekar,* A. Ramamoorthy,* and R. J. Wittebort†

*Department of Chemistry, Biophysics Research Division, and Macromolecular Science and Engineering, University of Michigan, 930 North University Avenue, Ann Arbor, Michigan 48019-1055; and †Department of Chemistry, University of Louisville, 2320 S. Brook Street, Louisville, Kentucky 40292

**Chemical shift anisotropy (CSA) is an immensely useful interaction to study the structure, dynamics, and function of a wide variety of chemical and biological molecules. Traditionally the only unambiguous way to determine both the principal values and the orientation of the principal axes of the CSA tensor has been to follow the chemical shift frequency changes as a crystal of known structure is rotated relative to the direction of the external magnetic field. This classic method employs rotations about three mutually orthogonal axes of a single crystal. It is shown here that just two, or one, of the above rotations suffice to determine the CSA tensor orientation by borrowing, the easy to obtain, principal values of CSA from an independent source. Methods for using two rotation patterns or even a single rotation pattern are described and illustrated with known chemical shielding tensors.** © 2002 Elsevier Science (USA)

*Key Words*: chemical shift anisotropy; shielding tensor; single crystal; rotation; solid-state NMR.

## INTRODUCTION

The chemical shielding tensor is an experimentally determined basic NMR parameter and highly valuable in understanding the nature of chemical bonding, structure, dynamics, and function of chemical and biological molecules (*1–8*). Its value lies in its ability to report on local chemical environment that in turn can be related to molecular conformation. The shielding tensor is a mathematical manifestation of the interaction of the local current density with an applied magnetic field $\mathbf{B_0}$, the outcome of which presents the immersed nuclear spin a local magnetic field different from $\mathbf{B_0}$. Nuclear spins with different local current densities, due to the variation in the chemical environment, thus see different local fields and this results in the resolution of resonance frequencies. The interaction in general is anisotropic; i.e., the relative orientation of $\mathbf{B_0}$ with respect to the local molecular geometry influences the resonance frequency. For example, in powder samples, where all orientational possibilities are realized, the classic powder pattern ensues (*1–3*). The interaction is historically known as chemical shift anisotropy (CSA) (*3*).

The CSA interaction is a second rank tensor with a nonzero trace (*1–3*). It is a symmetric $3 \times 3$ matrix in the Cartesian repre-

sentation and has six independent matrix elements. This matrix can be transformed to a principal axis system (PAS), wherein the only nonzero elements are the principal values of the tensor lying on the diagonal. The three Euler angles of an orthogonal transformation and the three principal elements of the CSA tensor, or equivalently the six independent elements of the nondiagonal matrix, represent the CSA tensor and its orientation in the molecular frame.

Though the CSA interaction originates from current densities in a molecule, it is inaccessible even to X-ray crystallography that is sensitive to charge densities. The tensor elements or their various combinations can be obtained from NMR experiments. For example, common solution NMR experiments report the isotropic chemical shift, which is equal to one third of the trace of the tensor matrix in any frame. On the other hand, the principal elements can be readily and accurately determined from the positions of the shoulders of the experimental powder pattern spectrum of a polycrystalline sample obtained using solid-state NMR methods (*2, 3*). However, the bounty of choices available to determine isotropic shifts and principal values drastically dwindles to a handful of difficult and laborious techniques when the orientation of the CSA tensor in the molecular frame is sought. The tensor orientation can be determined from one- or two-dimensional, static or magic angle spinning (MAS), NMR experiments of powder samples that convolute, or correlate, CSA and dipolar interactions (*9–16*). However, these techniques rely on favorable sample and experimental conditions and therefore seldom provide full information about the CSA tensor orientation. The only method that ensures finding the complete tensor orientation is the celebrated technique of analyzing single crystal NMR "rotation patterns" (*1–3, 17–22*). The orientation in the crystal frame is rigorously determined and, with an X-ray structure, molecular orientation is determined as well if the unit cell contains a single molecule (or all molecules in the unit cell, translations aside, are related by a center of inversion). Otherwise, assignment of molecular orientations to the structurally equivalent but magnetically nonequivalent sites requires additional information. However, single crystal NMR comes with a price. Even when in possession of high quality crystals, the method is tedious and very unforgiving to experimental and

analysis errors. Stringent requirements must be met at every stage. It involves recording NMR spectra at many orientations as the crystal is rotated about three mutually perpendicular axes. The rotation axes should be strictly held orthogonal to $\mathbf{B_0}$. It is also necessary to know the zero or starting points common to pairs of rotation patterns. With an eye toward one of the most important applications, namely solid-state NMR of biological molecules, it must be kept in mind that obtaining large size crystals of biological molecules is difficult. This results in poor signal to noise ratio spectra increasing experimental uncertainties. Any means to reduce the length of the procedure immediately translates into savings in terms of labor, time, and error reduction. It is also possible to obtain the tensor orientation by a single rotation about an axis that is not orthogonal to $\mathbf{B_0}$ (*1*). However, this is not the conventional choice. This may be because of difficulty of defining such an axis with confidence. The classic method of three rotations however offers many checks that can be used for verification of the experimental procedure. For example, there is at least one orientation for which the spectra are identical for any pair of the 3 orthogonal rotations. Another check that is not available to an arbitrary rotation axis is the $\pi$ periodicity of the spectra with respect to the rotation angle in the classic method.

Principal values of the tensor are very easy to determine compared to the characterization of the full tensor, and a crystal is not needed. Many methods are available to determine the principal values, the most obvious being reading them off of a powder spectrum. The sideband analysis of MAS spectra is another popular method (*23*). Below we describe a strategy, by using independently determined principal values of the tensor, to reduce the number of required rotations in the conventional method to (*1*) just two to obtain an unambiguous determination of the tensor orientation and (*2*) or even one to obtain four candidates for the tensor orientations. Furthermore, this number can be reduced with the same approaches used for assigning tensor molecular orientations to structurally equivalent but magnetically nonequivalent sites.

## THEORY

In the Cartesian representation, the shielding tensor is a symmetric $3 \times 3$ matrix and is diagonal in its PAS (frame $P$). In the conventional single crystal method of analyzing experimental rotation patterns about three mutually orthogonal axes, all the distinct matrix elements (three diagonal and three off-diagonal) are determined in some well-defined frame (such as a crystal based orthogonal coordinate system) (*2, 3*). Let us denote this shielding tensor in the crystal frame as $\sigma$ which can be diagonalized to obtain $\sigma^P$ by the following unitary transformation

$$\sigma = \mathbf{R}^T \sigma^P \mathbf{R}, \qquad [1]$$

where $\mathbf{R}$ is an orthogonal transformation between the $P$ and crystal frames, while $\mathbf{R}^T$ is its transpose. $\mathbf{R}$ can be given in terms of Euler angles, $\Omega = (\alpha, \beta, \gamma)$, by

$$\mathbf{R}(\Omega) = \mathbf{R}_z(\alpha)\mathbf{R}_y(\beta)\mathbf{R}_z(\gamma). \qquad [2]$$

Each of the three conventional single crystal rotations yields two diagonal elements and one off-diagonal element of $\sigma$. For example, rotation about $<y|$ yields values of $\sigma_{XX}, \sigma_{ZZ}$, and $\sigma_{XZ}$. The union of the three sets of matrix elements yields the full $\sigma$ matrix, which is diagonalized to yield $\sigma^P$ and $\mathbf{R}$, and therefore the complete shielding tensor can be characterized in the crystal frame. On the other hand, if $\sigma^P$ (or the values of the principal elements $\sigma_{11}, \sigma_{22}$, and $\sigma_{33}$) is known then the matrix elements of $\sigma$ are functions of the Euler angles $(\alpha, \beta, \gamma)$ only. Therefore, the task of completely characterizing the shielding tensor is reduced to determining only the values of these three angles. In this study, we discuss two independent methods to determine the values of $(\alpha, \beta, \gamma)$ angles. Examples illustrating the application of these two methods using reported shielding tensors are presented in the next section.

### Method I

The values of $(\alpha, \beta, \gamma)$ angles can be determined by solving three equations that are generated from any one of the single crystal rotation experimental data. However, the equations are nonlinear and trigonometric in the dependency of the three unknown parameters. There is no *a priori* guarantee that solutions exist for these equations. On the other hand, 4 of the 6 distinct $\sigma$ matrix elements (2 diagonal and 2 off diagonal) determined from two conventional experimental rotation data provide 4 equations with only 3 unknown parameters; this provides the needed nudge to get over the mathematical hump to yield the complete tensor. By searching the space of the three Euler angles and using 4 above mentioned equations, we can determine the values of $(\alpha, \beta, \gamma)$ angles that define the orientation of the shielding tensor in the molecular frame.

### Method II

An algebraic method, in contrast to the Euler angle search approach used above, is now described. The starting point is the secular equation which is typically solved for the eigenvalues, $\sigma_{ii}^{PAS}$.

$$\begin{vmatrix} \sigma_{11} - \sigma_{jj}^P & \sigma_{12} & \sigma_{13} \\ \sigma_{12} & \sigma_{22} - \sigma_{jj}^P & \sigma_{23} \\ \sigma_{13} & \sigma_{23} & \sigma_{33} - \sigma_{jj}^P \end{vmatrix} = 0, \quad j = 1, 2, 3. \quad [3]$$

Since the eigenvalues are known here, it can be solved to determine the values of the unknown off-diagonal elements. Three simultaneous nonlinear equations are obtained,

$$\begin{aligned} &\left(\sigma_{xx} - \sigma_{jj}^P\right)\sigma_{yz}^2 + \left(\sigma_{yy} - \sigma_{jj}^P\right)\sigma_{xz}^2 + \left(\sigma_{zz} - \sigma_{jj}^P\right)\sigma_{xy}^2 - 2\sigma_{xz}\sigma_{yz}\sigma_{xy} \\ &- \left(\sigma_{xx} - \sigma_{jj}^P\right)\left(\sigma_{yy} - \sigma_{jj}^P\right)\left(\sigma_{zz} - \sigma_{jj}^P\right) = 0, \quad j = 1, 2, 3. \quad [4] \end{aligned}$$

When two off-diagonal elements are known, this approach gives the same results as the Euler angle search method outlined above, but involves nothing more than applying the quadratic equation either 2 or 3 times and choosing the common root. Subsequently, $\sigma$ is diagonalized to obtain the eigenvectors from which Euler angles can be determined if desired. To consider the possibility of reconstructing tensors from rotation about a single axis, we take (without loss of generality) this axis as $\langle y|$. Thus, the known off-diagonal element is $\sigma_{XZ}$ and the task is to determine $\sigma_{XY}$ and $\sigma_{YZ}$; conveniently done using any of the three possible pairs of Eq. [4] and a standard algorithm for solving simultaneous nonlinear equations (24). In practice, we find 4 discrete solutions related by symmetries in their orientations. Defining the eigenvector corresponding to a particular PAS component as $(x, y, z)$, the four solutions have vectors of the form $(x, y, z)$, $(x, -y, z)$, $(x', y, z')$, and $(x', -y, z')$. In some cases, only two solutions with eigenvector symmetries $(x, y, z)$, $(x, -y, z)$ are found. Approaches for selecting the correct orientation are discussed in the next section.

## RESULTS AND DISCUSSION

We now illustrate these two methods with examples. First, using shielding tensors reported in the literature (18–20) summarized in Table 1, we use the Euler angle search to confirm that, given a shielding tensor and its eigenvalues, one can uniquely "reconstruct" the tensor orientation when rotation data from any 2 of the three axes is combined with accurate principal components. Next, we discuss approaches for selecting the correct tensor orientation (of 4 choices) inherent to the reconstruction based on a single axis rotation.

This Euler angle search method was implemented as a computer algorithm as follows:

1. Orientational space described by the Euler angles was divided into a grid of one-degree intervals with $0 \leq \alpha \leq \pi$, $0 \leq \beta \leq \pi$ and $0 \leq \gamma \leq 2\pi$ in order to search the orientation of the tensor in the crystal frame. The range for the $\alpha$ angle was halved because $\mathbf{R}_z(\alpha + \pi)^T \sigma^P \mathbf{R}_z(\alpha + \pi) = \mathbf{R}_z(\alpha)^T \sigma^P \mathbf{R}_z(\alpha)$.

2. At each grid point, $\mathbf{R}$ was generated and the similarity transformation given by Eq. [1] applied to obtain the calculated shielding matrix, $\sigma_{calc}$.

3. The common subset of four elements (2 diagonal and 2 off-diagonal elements) between the source tensor (constructed using experimental data) and the calculated tensor was chosen to compute the sum of squares of differences between corresponding elements.

4. Euler angles corresponding to the minimum sum of squares of deviations were chosen.

The results obtained from this study are presented in Table 2. The orientations of CSA tensors obtained from 4 distinct elements (two rotations in combination with the principal components) are as good as the values determined from the conventional three rotation patterns. Even for the worst cases, the $C_1$, $C_2$, and $C_4$ carbons of L-threonine, orientation of the tensor determined from different combinations of rotation patterns differ not more than by a couple of degrees. Trigonometric symmetry of the Euler rotation, Eq. [2], gives two orientations each for $C_2$ and $C_4$ carbons of L-threonine (within a degree or two margin mentioned above) which are completely equivalent; i.e., the respective tensors in the crystal frame for the two orientations are identical. Importantly, this shows that the orientations obtained from all combinations of pairs of rotation experiments are equivalent, i.e., the procedure is not sensitive to the choice of the rotation axes.

We now consider the case where the crystal is rotated about a single axis orthogonal to $\mathbf{B_0}$. In addition to further reducing experimental time, this approach circumvents two technical problems associated with single crystal studies: inaccuracies associated with mounting the crystal accurately in 3 orthogonal orientations and adjusting the NMR coil geometry or size to accommodate arbitrary orientations of crystal morphologies like needles. The primary disadvantage is that the tensor orientation is not uniquely determined (there are four possibilities). Also, errors in the eigenvalues are propagated into the tensor orientation and this is discussed below.

## TABLE 1
### Test Shielding Tensors Taken from the Literature

| Mol. | Site | Ref. | $\sigma_{xx}$ | $\sigma_{xy}$ | $\sigma_{xz}$ | $\sigma_{yy}$ | $\sigma_{yz}$ | $\sigma_{zz}$ | $\sigma_{xx}^P$ | $\sigma_{yy}^P$ | $\sigma_{zz}^P$ | $\alpha,\ \beta,\ \gamma$ |
|---|---|---|---|---|---|---|---|---|---|---|---|---|
| Gly | $C_2$,1 | 18 | 85.8 | 6.5 | −9.8 | 65.2 | 4.0 | 96.1 | 62.0 | 83.0 | 102.0 | 113, 149, 180 |
| Gly | $C_2$,2 | 18 | 85.8 | −6.5 | −9.8 | 65.2 | −4.0 | 96.1 | 62.0 | 83.0 | 102.0 | 113, 31, 0 |
| GG | $C_1$ | 19 | −29.7 | 55.7 | −38.1 | −79.4 | −21.0 | −14.6 | −115.6 | −48.6 | 40.6 | 87, 52, 328 |
| GG | N | 19 | 119.9 | −24.9 | 70.8 | 50.9 | −26.6 | 94.3 | 33.0 | 43.6 | 188.6 | 165, 129, 19 |
| Thr | $C_1$ | 20 | 209.2 | 47.3 | −19.9 | 127.3 | −16.4 | 173.4 | 105.0 | 164.7 | 240.2 | 84, 110, 154 |
| Thr | $C_2$ | 20 | 57.2 | −2.8 | 1.6 | 64.9 | 6.6 | 58.4 | 52.6 | 58.9 | 69.0 | 144, 120, 261 |
| Thr | $C_3$ | 20 | 50.7 | −14.5 | 9.1 | 72.5 | 9.9 | 73.0 | 83.4 | 74.1 | 38.8 | 51, 110, 151 |
| Thr | $C_4$ | 20 | 23.1 | 0.0 | −4.6 | 23.0 | 13.2 | 10.5 | 32.1 | 23.1 | 1.4 | 1, 147, 71 |

*Note.* Principal components and Euler angles were accurately calculated numerically for each tensor. GG = glygly.

## TABLE 2
### Euler Angle Search Applied to Table 1 Data

| Mol. | Site | Axes used | $(\alpha, \beta, \gamma)$ | Mol. | Site | Axes used | $(\alpha, \beta, \gamma)$ |
|------|------|-----------|---------------------------|------|------|-----------|---------------------------|
| Gly | $C_2$, #1 | $a^*, b, c$ (exact) | 113, 149, 180 | Thr | $C_1$ | $a, b, c$ (exact) | 84, 111, 154 |
| " | $C_2$, #1 | $a^*, b$ | 113, 149, 180 | " | | $a, b$ | 84, 110, 154 |
| " | $C_2$, #1 | $b, c$ | 113, 149, 180 | " | | $b, c$ | 82, 111, 154 |
| " | $C_2$, #1 | $c, a^*$ | 113, 149, 180 | " | | $c, a$ | 84, 111, 154 |
| " | $C_2$, #2 | $a^*, b, c$ | 113, 31, 0 | " | $C_2$ | $a, b, c$ (exact) | 144, 120, 261 |
| " | $C_2$, #2 | $a^*, b$ | 113, 31, 0 | " | | $a, b$ | 144, 120, 261 |
| " | $C_2$, #2 | $b, c$ | 113, 31, 0 | " | | $b, c$ | 37, 60, 81 |
| " | $C_2$, #2 | $c, a^*$ | 113, 31, 0 | " | | $c, a$ | 37, 60, 81 |
| GG | $C_1$ | $a^*, b, c$ (exact) | 87, 52, 38 | " | $C_3$ | $a, b, c$ (exact) | 51, 110, 151 |
| " | $C_1$ | $a^*, b$ | 87, 52, 38 | " | | $a, b$ | 51, 110, 151 |
| " | $C_1$ | $b, c$ | 87, 52, 38 | " | | $b, c$ | 51, 110, 151 |
| " | $C_1$ | $c, a^*$ | 87, 52, 38 | " | | $c, a$ | 51, 110, 151 |
| " | N | $a^*, b, c$ (exact) | 165, 129, 19 | " | $C_4$ | $a, b, c$ (exact) | 1, 147, 71 |
| " | N | $a^*, b$ | 165, 129, 19 | " | | $a, b$ | 1, 147, 71 |
| " | N | $b, c$ | 165, 129, 19 | " | | $b, c$ | 1, 147, 71 |
| " | N | $c, a^*$ | 165, 129, 19 | " | | $c, a$ | 0, 33, 289 |

*Note.* Euler angles determined from rotation about any two crystal axes are compared with those computed from exact numerical diagonalization of the experimentally determined tensor.

Regarding selection of the correct solution, the choice to be made is similar to the commonly encountered problem in which the unit cell contains more than a single structurally equivalent but magnetically nonequivalent molecule, i.e., symmetry related shielding tensors. If, for example, the symmetry operation is a mirror-plane perpendicular to $y$, then the situation is equivalent to half of the choices here: two tensors with eigenvectors related by $(x, y, z)$ and $(x, -y, z)$. In many cases the number of possibilities is further multiplied if the rotation axes are the crystallographic axes (or a closely related orthogonal frame such as $(a^*, b, c)$ since the choice of how to combine rotation data from different axes for the chemically equivalent, magnetically nonequivalent sites is not unique. For amino acid carbons, these ambiguities have been resolved by the following experimentally realized local symmetry rules (7, 14, 18–22):

1. For carboxyl or carboxylate groups, the downfield (least shielded) component is along the $C–CO_2$ bond and the upfield (most shielded) component is along the normal to the plane of the $C–CO_2$ group.

2. For peptide carbonyl carbons ($C_1$), the most shielded component is along the peptide $OC_1N$ plane normal and the intermediate component is close ($\sim15°$) to the carbonyl bond.

3. For hydroxyl carbons, the downfield component is along the C–O bond,

4. For amino acid $\alpha$-carbons ($C_2$), the most downfield component is along the $C_1C_2N$ plane normal and the intermediate component bisects the $C_1$–$C_2$–N angle.

5. For methyl groups, the most shielded component is along the $C–CH_3$ bond.

Table 3 summarizes the results when the possible orientations generated by single axis analysis of the $^{13}C$ data from Table I

are compared to the relevant reference vector(s) described above. Listed are the angular deviations from the reference vectors calculated directly from the scalar product (direction cosine) of the two vectors compared. When the relevant rule specifies all 3 PAS component orientations (1, 2, and 4 above), the value listed is the average of the 3 angles. Small angles indicate that the solution is close to the symmetry rule. Since the correct orientation is known here, it is labeled $(x, y, z)$ in Table 3. In all cases, the correct orientation has the smallest deviation. In three cases, a second solution is close, but two of these spurious solutions would likely be eliminated if the rules for hydroxyl and methyl carbons specified the molecular orientations of 3 rather than a single shielding tensor component.

The effect of experimental errors in the principal components (eigenvalues) on the tensor orientation is determined by

## TABLE 3
### Angular Differences between Tensor Orientations Based on Single Axis Rotation Data (Table I) and Standard Symmetry Rules (See Text)

|  | $(x, y, z)$ | $(x, -y, z)$ | $(x', y, z')$ | $(x', -y, z')$ |
|--|-------------|--------------|----------------|-----------------|
| Gly $C_2$ #1 | 12° | 41° | — | — |
| Gly $C_2$ #2 | 12° | 41° | — | — |
| GlyGly $C_1$ | 10° | 48° | 43° | 32° |
| Thr $C_1$ | 2° | 7° | 33° | 34° |
| Thr $C_2$ | 5° | 47° | 41° | 58° |
| Thr $C_3$ | 4° | 58° | 58° | 8° |
| Thr $C_4$ | 5° | 8° | 60° | 60° |

*Note.* Rules for $C_1$ and $C_2$ carbons specify 3 PAS component orientations (see text) and the value listed is the average of the 3 angles between the eigenvectors and the reference vectors. The correct orientation, known here, is labeled $(x, y, z)$. Only two tensor orientations were found for Gly $C_2$.
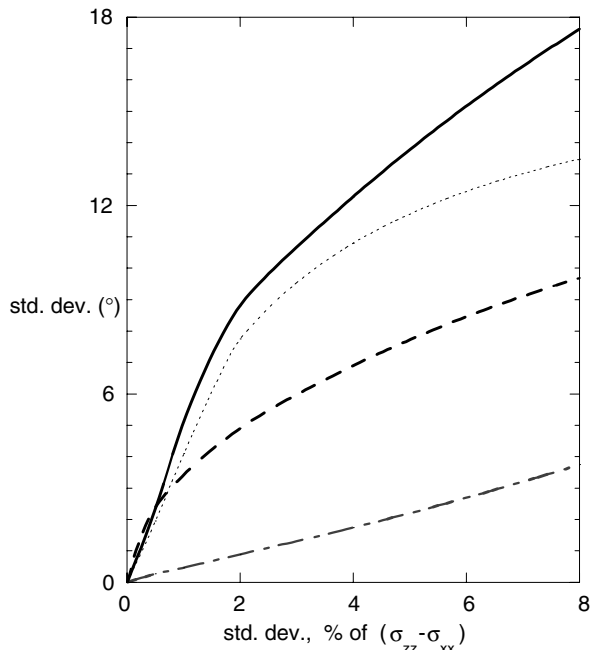
**FIG. 1.** Standard deviation in eigenvector orientations (degrees) as a function of standard deviation in principal components (percent of $\sigma_{zz} - \sigma_{xx}$). The curves are as follows: axially symmetric tensor with the unique axis parallel (solid line), perpendicular (dashed line), and at $45°$ (dashes and dots) relative to the crystal rotation axis. Also shown, an arbitrarily oriented axially asymmetric tensor (dots). Uncertainties for the two other components, not shown, are smaller.

Monte Carlo simulation as follows: Given the eigenvalues and their standard deviations, the eigenvectors (tensor orientation) are determined for a large number ($\sim 10^3$) of randomly generated principal components satisfying a normal distribution with the specified standard deviations (25). The changes in the three eigenvector orientations are calculated for each randomly generated set of principal components and their standard deviations are calculated for the simulation. Figure 1 shows how standard deviations in eigenvector orientations vary with standard deviations in the principal components for several illustrative cases: an axially symmetric tensor with the unique axis perpendicular, parallel or at $45°$ relative to the rotation axis and an axially asymmetric tensor ($\eta = 1$) tensor with an arbitrary orientation relative to the rotation axis. When the tensor is axially symmetric, the orientation is specified completely by the eigenvector of the unique component. Uncertainties in this orientation are largest and smallest, respectively, when the rotation and tensor axes are parallel and separated by $45°$. For the asymmetric case, all three vector orientations are needed and the largest uncertainty (from the vector corresponding to $\sigma_{yy}$) is less than but comparable to the worst axial case. In summary, typical errors in the principal components, $\leq 2\%$, correspond to uncertainties in the orientations of $\leq 6°$.

## CONCLUSIONS

NMR rotation patterns of a single crystal are the celebrated method to obtain the orientation of the chemical shielding tensor in the crystal frame unambiguously. Though almost any amount of labor and cost would be tolerated for such pristine information, not even measurable by X-ray crystallographic methods, any methods for reducing the cost (in terms of labor, time, and error) would be highly welcome. In this study we have shown that, by using independently and much more easily determined principal values of the chemical shielding tensor, the number of "classic" single crystal rotation patterns required can be cut down from three to two. Even in the event one chooses to employ all the three classic rotations, since the analysis can be carried out independently about any pair of axes, the number of helpful checks available aids the analysis to obtain the tensor orientation. We have also described a method using a single rotation. In general, four tensor orientations are found and the problem of eliminating the spurious orientations is the same as is frequently encountered when determining tensor molecular orientations in samples with magnetically nonequivalent but structurally equivalent sites. Applying the same symmetry rules used to resolve this ambiguity is successful in eliminating most of the spurious orientations. More refined rules based on a larger data base of shielding tensors and *ab initio* calculations should improve the viability of this approach. We expect it will be fruitful in cases where there are practical problems for rotation about 2 or 3 orthogonal axes.

## REFERENCES

1. U. Haeberlen, "Advances in Magnetic Resonance: Supplement 1." Academic Press, San Diego, 1976; M. Mehring, "High Resolution NMR of Solids." Springer-Verlag, Berlin, 1983.

2. K. Schmidt-Rohr and H. W. Spiess, "Multidimensional Solid State NMR and Polymers." Academic Press, London, 1994.

3. D. M. Grant, "Encyclopedia of Nuclear Magnetic Resonance" (D. M. Grant and R. K. Harris, Eds.), Vol. 6, pp. 1298–1321. Wiley, New York, 1996.

4. A. C. de Dios and E. Oldfield, *J. Am. Chem. Soc.* **116,** 11,485–11,488 (1994); A. C. de Dios, J. G. Pearson, and E. Oldfield, *Science* 1491–1496 (1993).

5. D. K. Lee, R. J. Wittebort, and A. Ramamoorthy, *J. Am. Chem. Soc.* **120,** 8868–8874 (1998); A. Shoji, A. Ando, S. Kuroki, I. Ando, and G. A. Webb, *Annu. Rep. NMR Spectrosc.* **26,** 55–98 (1993); C. H. Wu, A. Ramamoorthy, L. M. Gierasch, and S. J. Opella, *J. Am. Chem. Soc.* **117,** 6148–6149 (1995).

6. J. R. Brender, D. M. Taylor, and A. Ramamoorthy, *J. Am. Chem. Soc.* **123,** 914–922 (2001); P. Rossi and G. Harbison, *J. Magn. Reson.* **151,** 1–8 (2001).

7. Y. Wei, D. K. Lee, and A. Ramamoorthy, *J. Am. Chem. Soc.* **123,** 6118–6126 (2001); M. Hong, *J. Am. Chem. Soc.* **122,** 3762–3770 (2000).

8. C. Scheurer, N. R. Skrynnikov, S. F. Leinin, S. K. Straus, R. Bruschweiler, and R. R. Ernst, *J. Am. Chem. Soc.* **121,** 4242–4251 (1999); K. J. Hallock, D. K. Lee, and A. Ramamoorthy, *J. Chem. Phys.* **113,** 11,187–11,193 (2000).

9. M. Linder, A. Hohener, and R. R. Ernst, *J. Chem. Phys.* **73,** 4959 (1980); R. K. Hester, J. L. Ackerman, V. R. Cross, and J. S. Waugh, *Phys. Rev. Lett.* **34,** 993 (1975).

10. M. G. Munowitz, W. P. Aue and R. G. Griffin, *J. Am. Chem. Soc.* **103,** 2529 (1982).

11. C. H. Wu, A. Ramamoorthy, and S. J. Opella, *J. Magn. Reson. A* **109,** 270–272 (1994).

12. M. H. Sherwood, D. W. Alderman, and D. M. Grant, *J. Magn. Reson.* **84,** 466–489 (1989).

13. J. M. Goetz and J. Schaefer, *J. Magn. Reson.* **129,** 222–223 (1997); J. Leppert, B. Heise, and R. Ramachandran, *J. Magn. Reson.* **145,** 307–314 (2000).

14. T. G. Oas, C. J. Hartzell, T. J. McMahon, G. P. Drobny, and F. W. Dahlquist, *J. Am. Chem. Soc.* **109,** 5957–5962 (1987); T. G. Oas, C. J. Hartzell, F. W. Dahlquist, and G. P. Drobny, *J. Am. Chem. Soc.* **109,** 5962–5966 (1987); C. J. Hartzell, M. Whitfield, T. G. Oas, and G. P. Drobny, *J. Am. Chem. Soc.* **109,** 5966–5969 (1987).

15. D. K. Lee and A. Ramamoorthy, *J. Magn. Reson.* **133,** 204–206 (1998).

16. M. Hong, J. D. Gross, C. M. Rienstra, R. G. Griffin, K. K. Kumashiro, and K. Schmidt-Rohr, *J. Magn. Reson.* **129,** 85–92 (1997).

17. E. Rivera, M. A. Kennedy, R. D. Admas, and P. D. Ellis, *J. Am. Chem. Soc.* **112,** 1400–1407 (1990); N. Takeda, S. Kuroki, H. Kurosu, and I. Ando, *Biopolymers* **50,** 61–69 (1999).

18. R. A. Haberkorn, R. E. Stark, H. van Willigen, and R. G. Griffin, *J. Am. Chem. Soc.* **103,** 2534–2539 (1981).

19. R. E. Stark, L. W. Jelinski, D. J. Ruben, D. A. Torchia, and R. G. Griffin, *J. Magn. Reson.* **55,** 266–273 (1983).

20. N. Janes, S. Ganapathy, and E. Oldfield, *J. Magn. Reson.* **54,** 111–121 (1983).

21. A. Pines, J. J. Chang, and R. G. Griffin, *J. Chem. Phys.* **61,** 1021 (1974).

22. A. Naito, S. Ganapathy, and C. A. McDowell, *J. Chem. Phys.* **74,** 3190 (1981).

23. J. Herzfeld and A. E. Berger, *J. Chem. Phys.* **73,** 6021 (1980).

24. W. H. Press, B. P. Flannery, S. A. Teukolsky, and W. T. Vetterling, "Numerical Recipes," Chap. 9. Cambridge University Press, Cambridge, UK, 1988.

25. P. R. Bevington and D. K. Robinson, "Data Reduction and Error Analysis for the Physical Sciences." McGraw–Hill, New York, 1992.